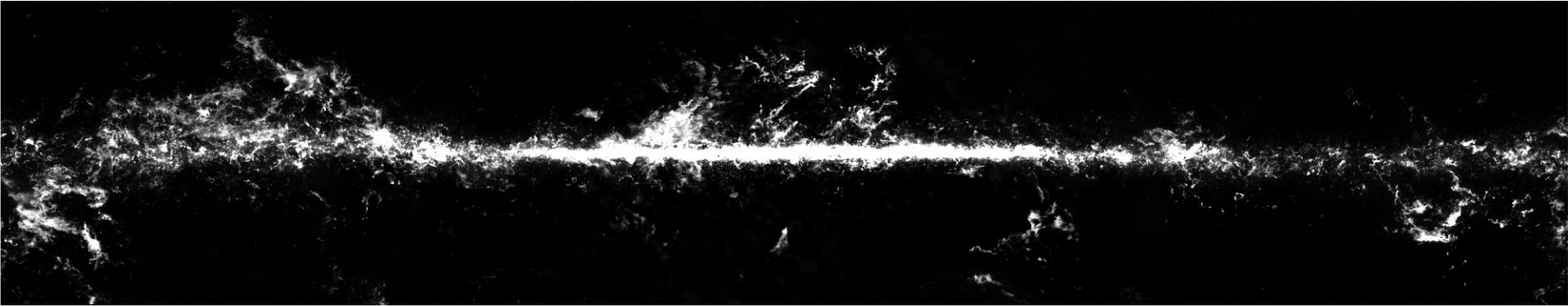


# Planck CO revisited

Improved maps of Galactic CO line emissions



**Shamik Ghosh (LBNL)** with Mathieu Remazeilles and Jacques Delabrouille

CMB-S4 Summer Collaboration Meeting 2024

*A&A vol 688 A64 / arXiv: 2312.07816*



# Motivation and context

- Next generation CMB experiments require improved models of Galactic emission.
- Improved models of Galactic foregrounds require improved maps of Galactic foreground.
- Current Galactic CO models are limited by the Planck CO data products.
- Our goal here is to produce low noise and low contamination full sky CO maps.
- Listen to Elisa Russier's talk tomorrow for an update on ongoing efforts to improve the thermal dust maps

# CO molecular line emission

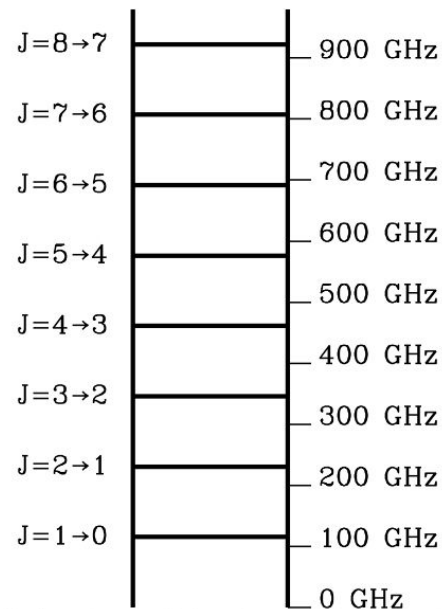
- CO is an asymmetric diatomic molecule with permanent electric dipole moment.

- Radiates at its rotational frequencies.

$$E_{\text{rot}} = \frac{J(J+1)\hbar^2}{2m_e r_e^2} \quad \Delta E_{J \rightarrow J-1} = \frac{J\hbar^2}{m_e r_e^2}$$

- The  $^{12}\text{C}^{16}\text{O}$  1-0 emission frequency is 115.271 GHz.
- CO maps we discuss here are in units of brightness temperature, integrated over relative velocity range ( $K_{\text{RJ}}$  km/s)

The CO Ladder

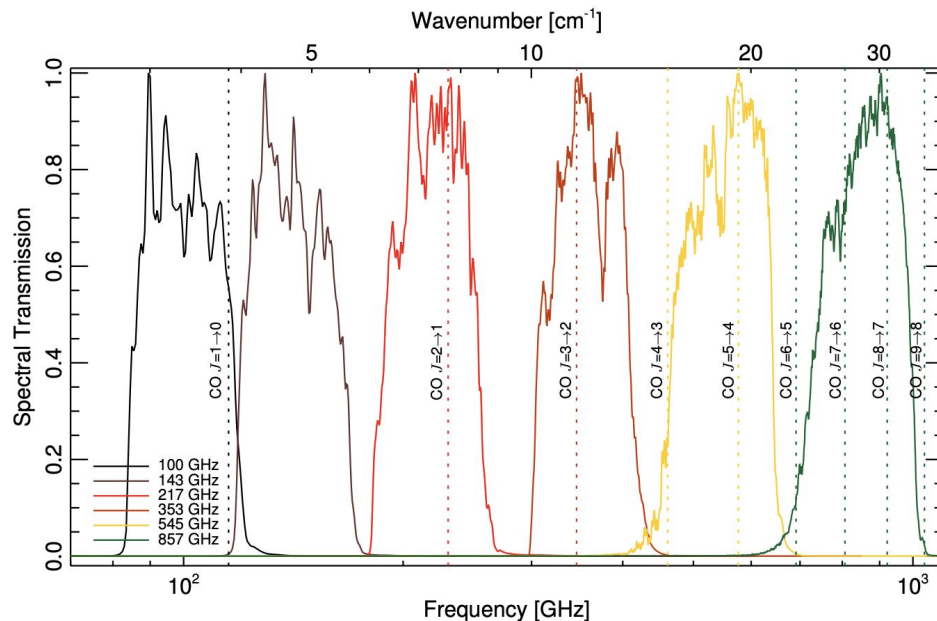


# CO line emission & Planck

Excellent sensitivity of the Planck HFI bolometers allow extraction of full sky galactic CO maps from Planck observations.

## Types of Planck CO data products:

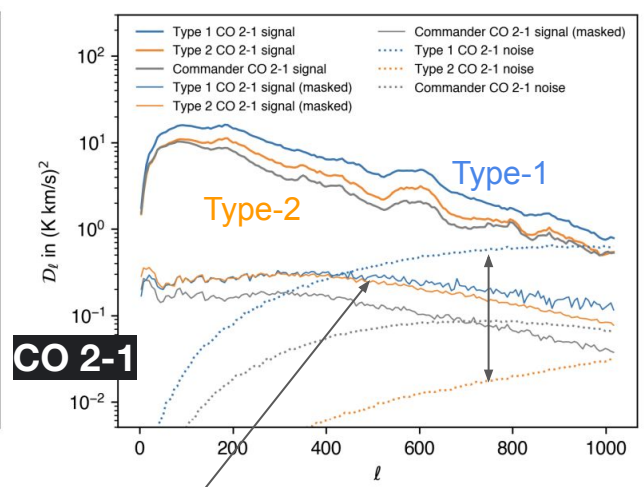
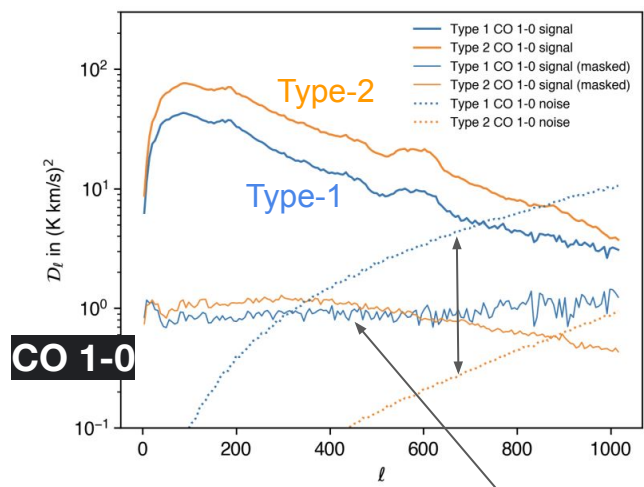
- Single frequency Type-1 CO maps ( $\text{CO}_{1-0}$ ,  $\text{CO}_{2-1}$ ,  $\text{CO}_{3-2}$ ): Noisy but low dust contamination.
- Multi-frequency Type-2 CO maps ( $\text{CO}_{1-0}$ ,  $\text{CO}_{2-1}$ ): High signal-to-noise but known to have dust contaminations.
- Multi-frequency Type-3 CO maps ( $\text{CO}_{1-0}$ ,  $\text{CO}_{2-1}$ ,  $\text{CO}_{3-2}$ )
- Commander CO map ( $\text{CO}_{2-1}$ )



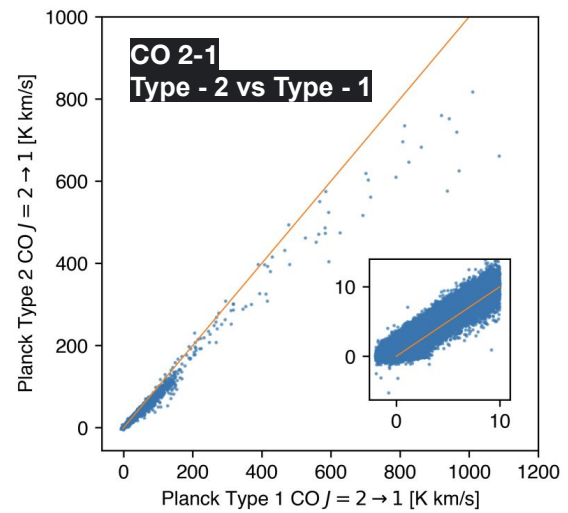
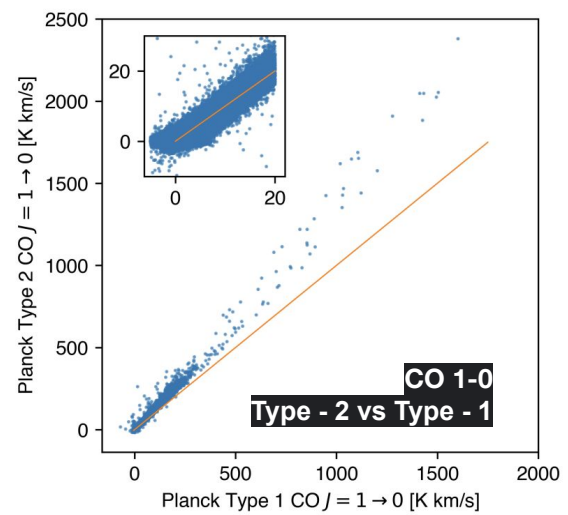
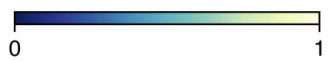
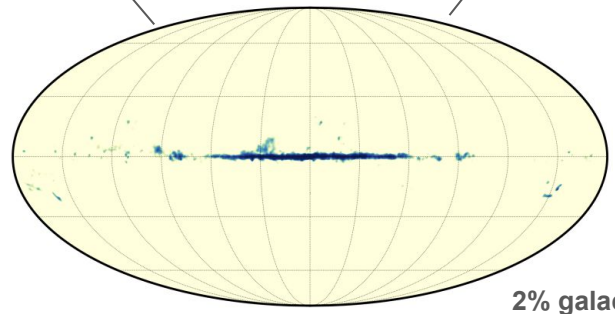
## Planck 2013 results. XIII. Galactic CO emission

Planck Collaboration: P. A. R. Ade<sup>90</sup>, N. Aghanim<sup>60</sup>, M. I. R. Alves<sup>60</sup>, C. Armitage-Caplan<sup>95</sup>, M. Arnaud<sup>75</sup>, M. Ashdown<sup>72,6</sup>, F. Atrio-Barandela<sup>19</sup>, J. Aumont<sup>60</sup>, C. Baccigalupi<sup>89</sup>, A. J. Banday<sup>98,10</sup>, R. B. Barreiro<sup>68</sup>, J. G. Bartlett<sup>169</sup>, E. Battaner<sup>100</sup>, K. Benabed<sup>61,97</sup>, A. Benoît<sup>58</sup>, A. Benoit-Lévy<sup>26,61,97</sup>, J.-P. Bernard<sup>10</sup>, M. Bersanelli<sup>36,51</sup>, P. Bielewicz<sup>98,10,89</sup>, J. Bobin<sup>75</sup>, J. J. Bock<sup>69,11</sup>, A. Bonaldi<sup>70</sup>, J. R. Bond<sup>9</sup>, J. Borrill<sup>14,92</sup>, F. R. Bouchet<sup>61,97</sup>, F. Boulanger<sup>60</sup>, M. Bridges<sup>72,6,64</sup>, M. Bucher<sup>1</sup>, C. Burigana<sup>50,34</sup>, R. C. Butler<sup>50</sup>, J.-F. Cardoso<sup>76,1,61</sup>, A. Catalano<sup>77,74</sup>, A. Chamballu<sup>75,16,60</sup>, R.-R. Chary<sup>77</sup>, X. Chen<sup>57</sup>, L.-Y. Chiang<sup>63</sup>, H. C. Chiang<sup>29,8</sup>, P. R. Christensen<sup>84,39</sup>, S. Church<sup>84</sup>, D. L. Clements<sup>36</sup>, S. Colombi<sup>61,97</sup>, L. P. L. Colombo<sup>55,62</sup>, G. Condon<sup>77</sup>, E. Couderc<sup>73</sup>, A. Coviello<sup>74</sup>, P. R. Cui<sup>109,86</sup>, A. Cuzco<sup>6,68</sup>, E. Cuttaia<sup>50</sup>

# Comparison of CO maps



Planck CO data products are not consistent with each other.



# Limitations of Type-1 CO maps

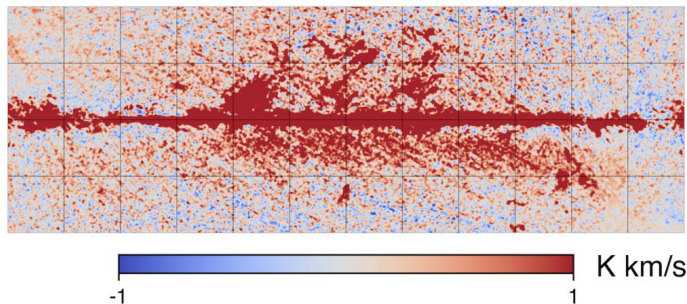
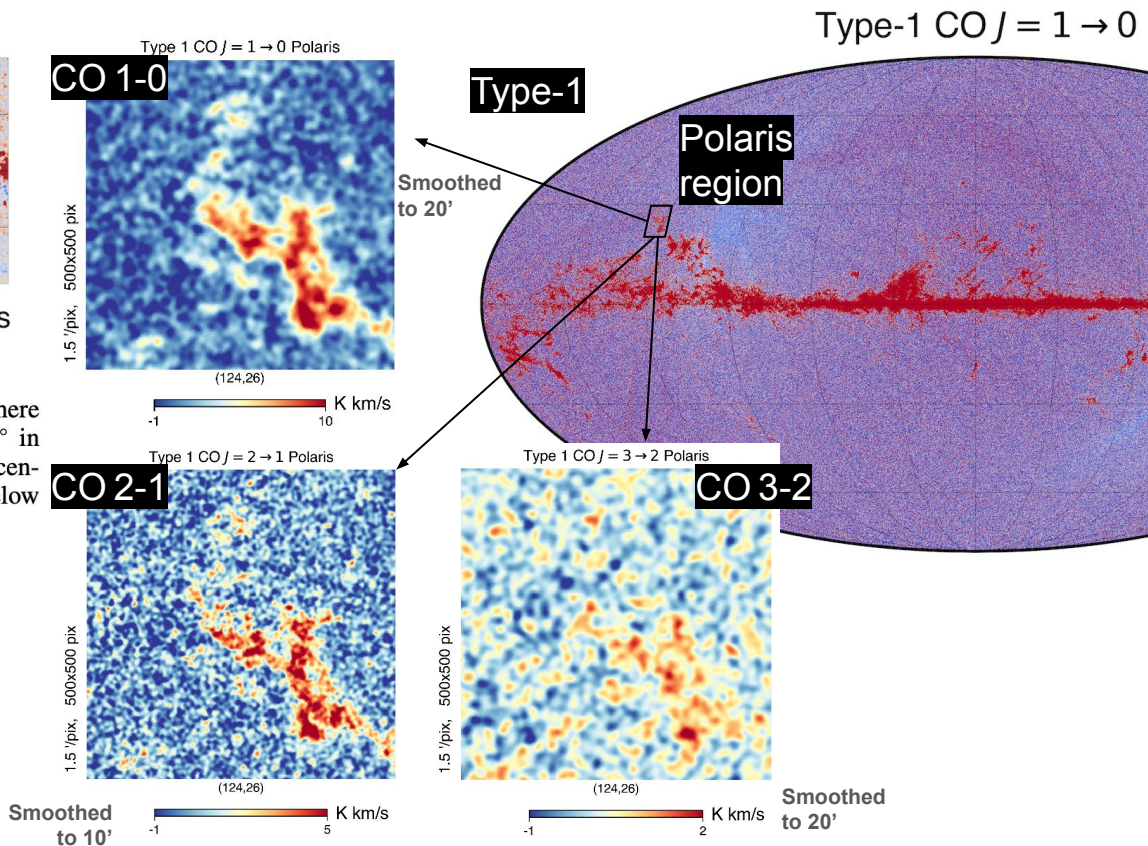
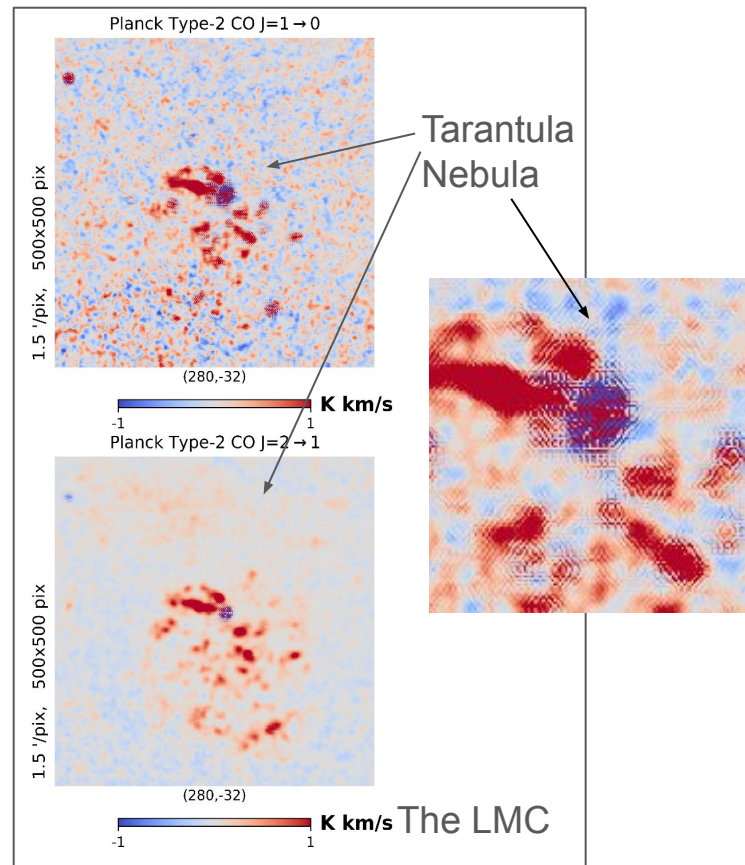
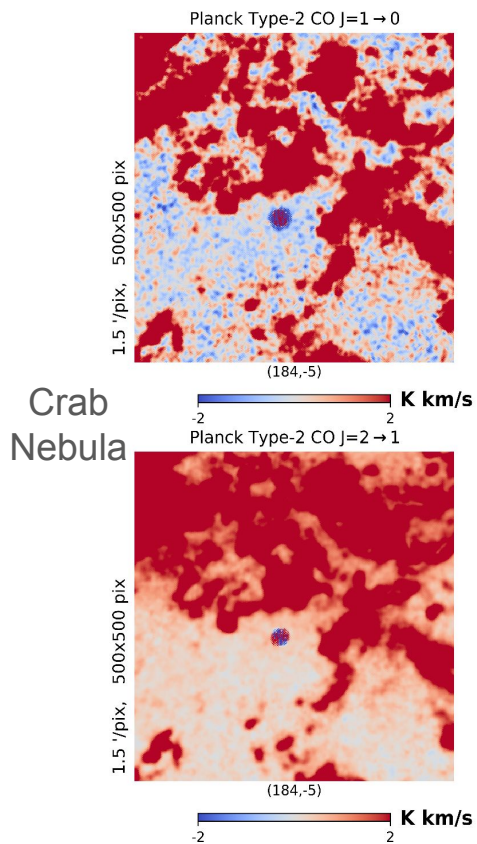
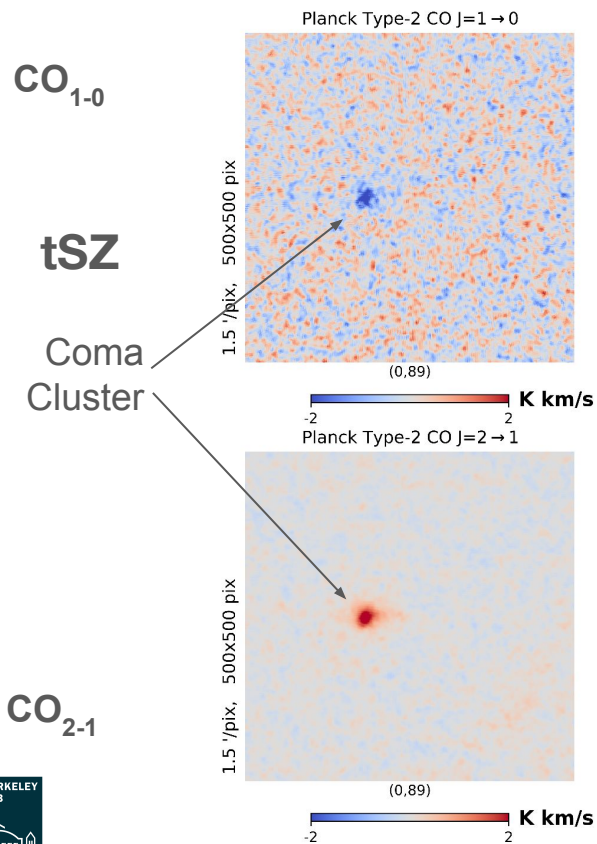


**Fig. 3.** The TYPE 1 CO  $J = 3 \rightarrow 2$  data product from Planck, shown here after smoothing to  $30'$  resolution. We are showing a region  $\pm 90^\circ$  in Galactic longitude and  $\pm 30^\circ$  in Galactic latitude about the Galactic center. Ringing effects and systematic residuals are visible above and below the Galactic ridge.

Low S/N for Type-1 maps.  
 $\text{CO}_{3-2}$  has systematic residuals



# Contamination in Type-2 maps



# Methodology

**Objective: Post-process existing Planck CO data products (Type-1 and Type-2) to produce improved new CO data products.**

Method outline:

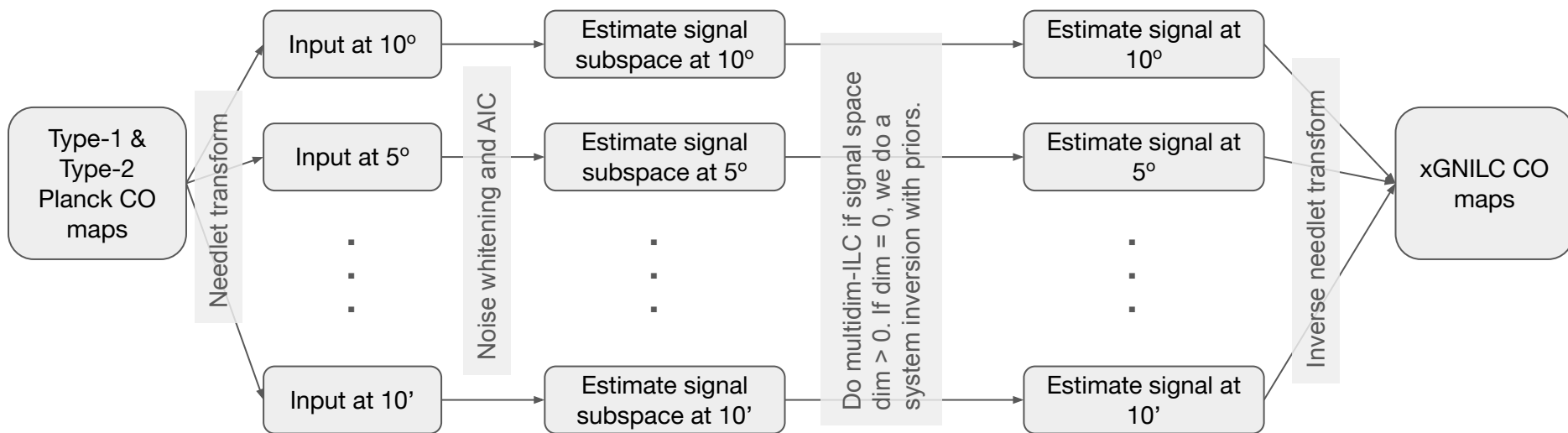
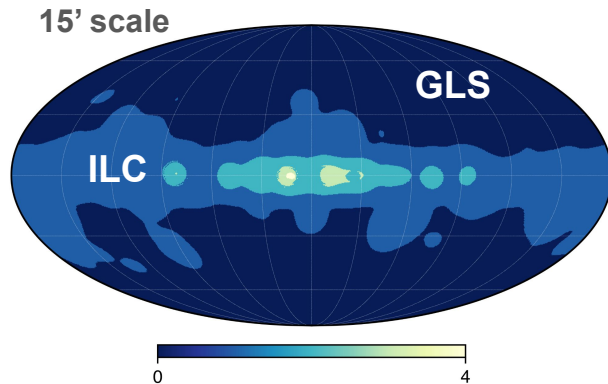
1. Use all Type-1 and Type-2 Planck CO maps (5 maps in total). Trust the Type-1 maps more.
2. Preprocess the Type-2 maps to remove compact and tSZ source contaminations.
3. Do a needlet transform to allow localization in harmonic and pixel domain.
4. Exploit the correlation between the three line emissions.
5. Use a prior on the CO line ratios but only when the S/N is poor.
6. Filter out systematics from the CO 3-2 map as a post-processing step.
7. Validate the new CO maps with independent CO observations (like Dame et al. 2001 and 2022).

**xGNILC**

We produce CO maps at NSIDE=1024 at 10 arcmin resolution.



# xGNILC pipeline



**Key difference with GNILC : retaining smaller scales where SNR is poor**

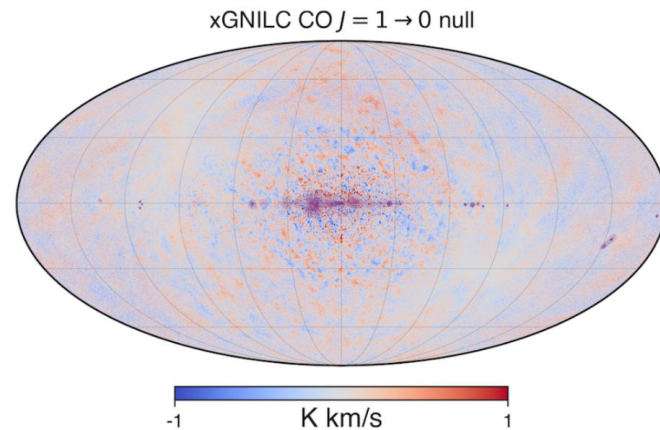
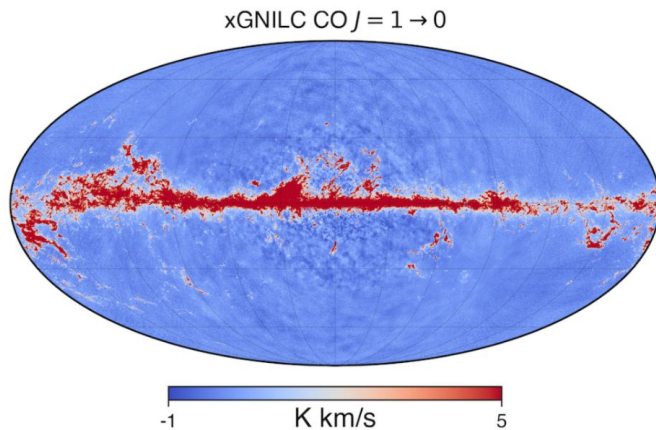
# Data products

- xGNILC CO map at  $N_{\text{side}} = 1024$  for CO  $J=1-0$ ,  $J=2-1$ , and  $J=3-2$  lines.
- Corresponding xGNILC CO jackknife noise maps.
- Systematic uncertainty maps for the xGNILC data product.
- 100 realizations of the projected noise for each xGNILC CO map.
- All the masks used in the analysis and confidence mask for the data product.
- Beam transfer function of xGNILC data products.

Data products are available from: [https://portal.nersc.gov/project/cmb/Planck\\_Revisited/co/](https://portal.nersc.gov/project/cmb/Planck_Revisited/co/)

# CO 1-0

CO  $J = 1-0$   
xGNILC



CO  $J = 1-0$   
Type-1

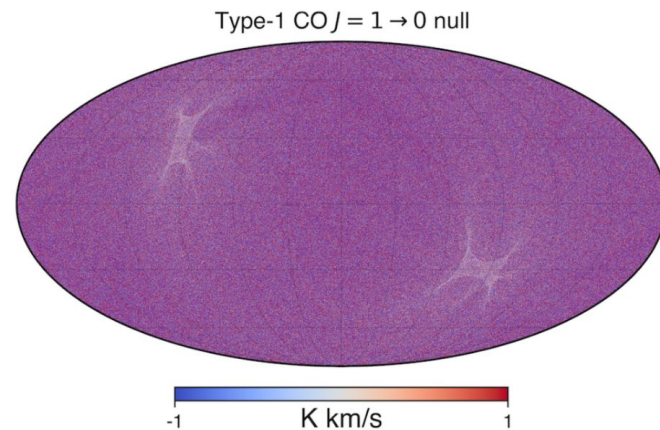
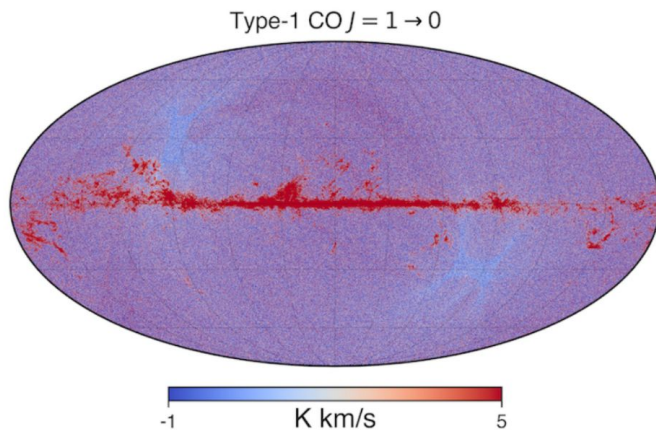
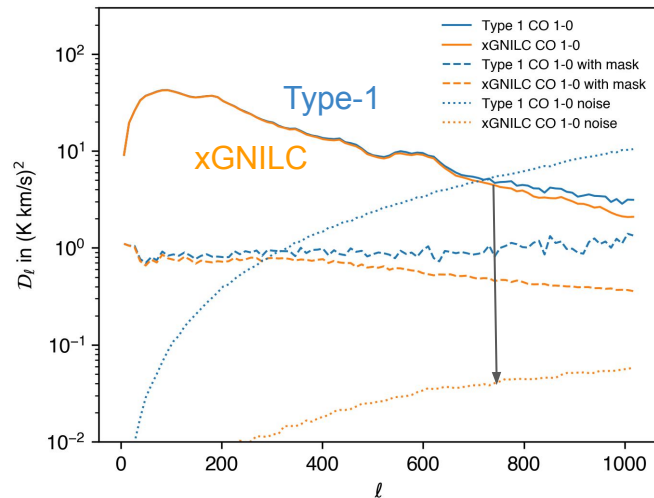
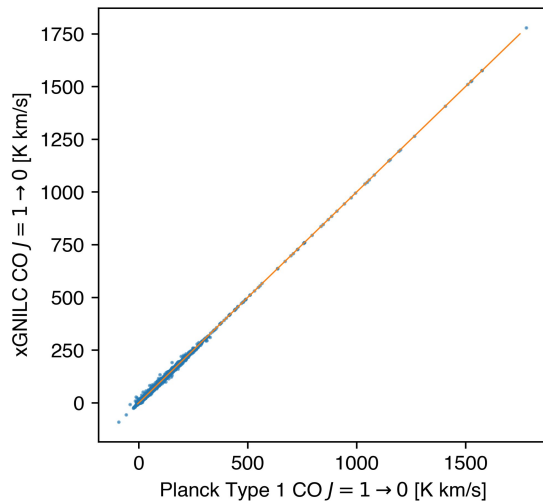


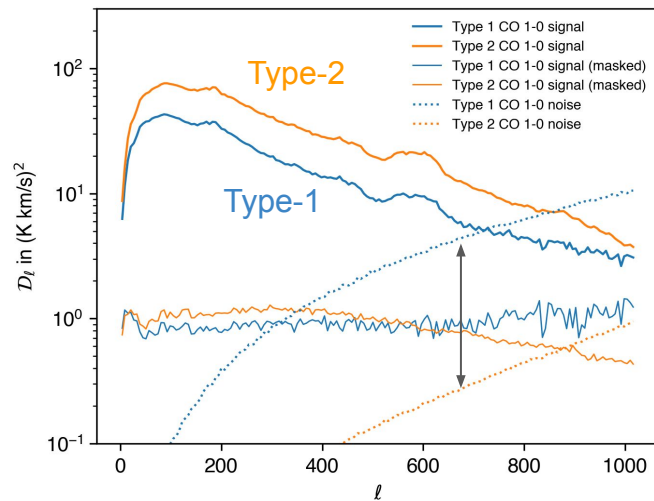
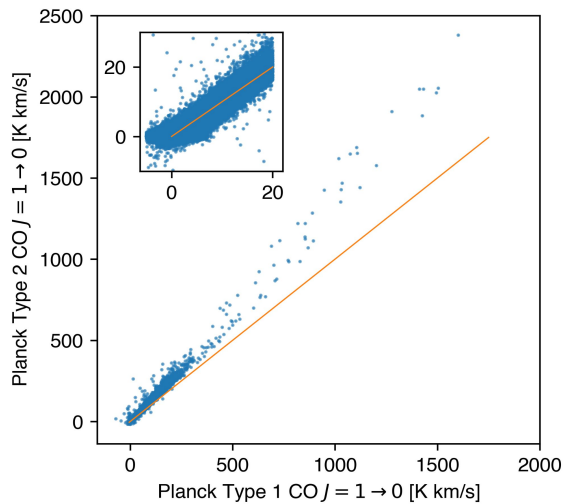
**Fig. 8.** Top: the xGNILC CO  $J = 1 \rightarrow 0$  map, at output resolution of  $10'$ , and the corresponding jackknife noise map. Bottom: Similar maps for the Planck TYPE 1 CO  $J = 1 \rightarrow 0$  data product, and the jackknife noise of the Planck TYPE 1 CO  $J = 1 \rightarrow 0$  map, both smoothed to  $10'$  resolution.

# CO 1-0

CO  $J = 1-0$   
xGNILC vs Type-1

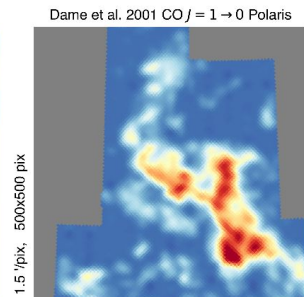
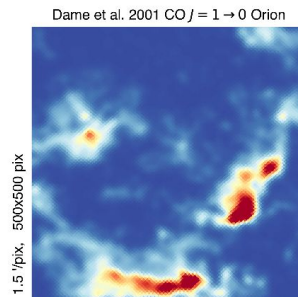
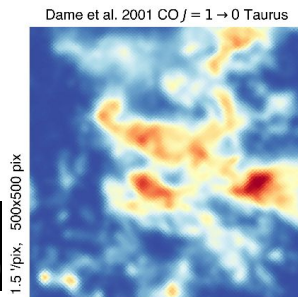


CO  $J = 1-0$   
Type-2 vs Type-1



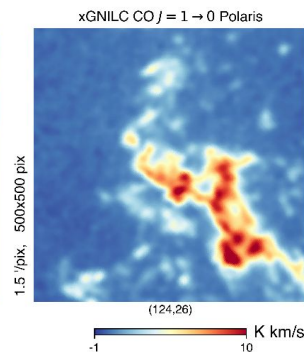
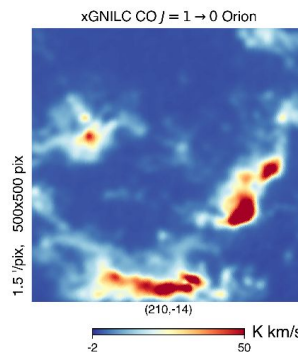
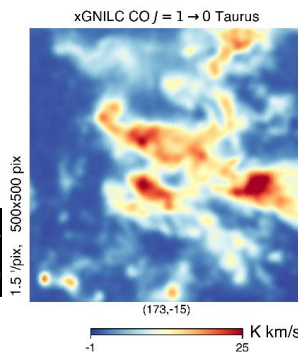
# CO 1-0

Dame et. al. 2001  
CO J=1-0

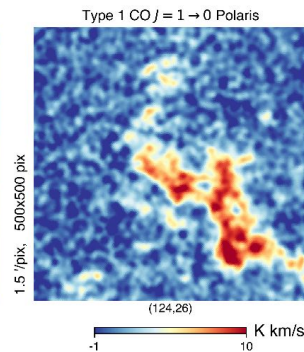
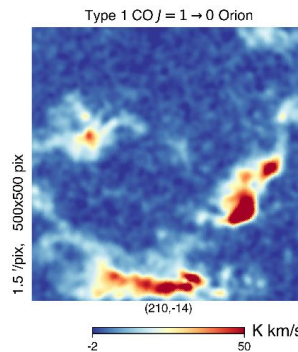
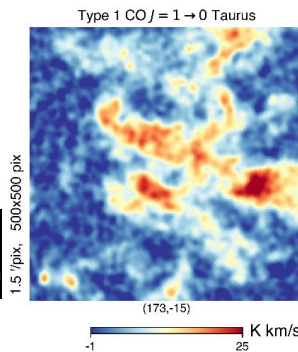


All maps  
smoothed to  
20 arcmin

xGNILC  
CO J=1-0



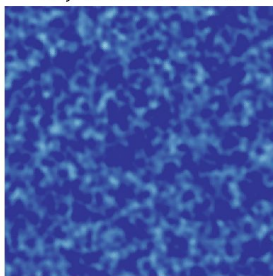
Type-1  
CO J=1-0



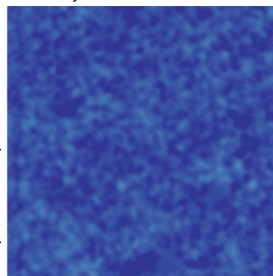
# CO 1-0

Type-1 - xGNILC  
CO J=1-0

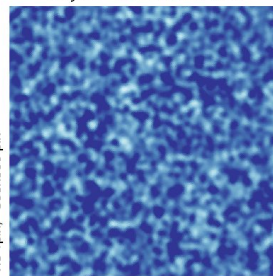
1.5 "/pix, 500x500 pix



1.5 "/pix, 500x500 pix



1.5 "/pix, 500x500 pix



K km/s

K km/s

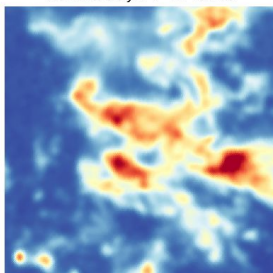
K km/s

xGNILC CO J = 1 → 0 Taurus

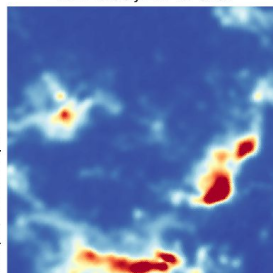
xGNILC CO J = 1 → 0 Orion

xGNILC CO J = 1 → 0 Polaris

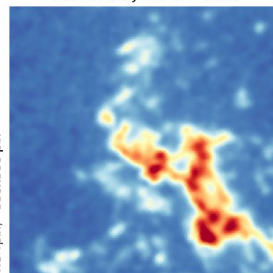
1.5 "/pix, 500x500 pix



1.5 "/pix, 500x500 pix



1.5 "/pix, 500x500 pix



K km/s

K km/s

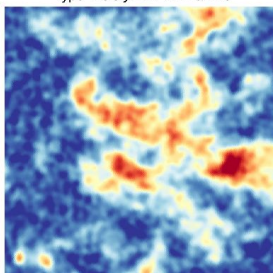
K km/s

All maps  
smoothed to  
20 arcmin

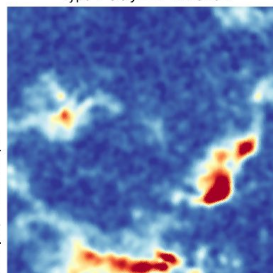
xGNILC  
CO J=1-0

Type-1  
CO J=1-0

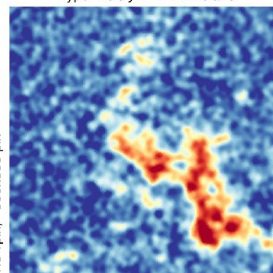
1.5 "/pix, 500x500 pix



1.5 "/pix, 500x500 pix



1.5 "/pix, 500x500 pix



K km/s

K km/s

K km/s

# CO 1-0

## High Latitude Clouds

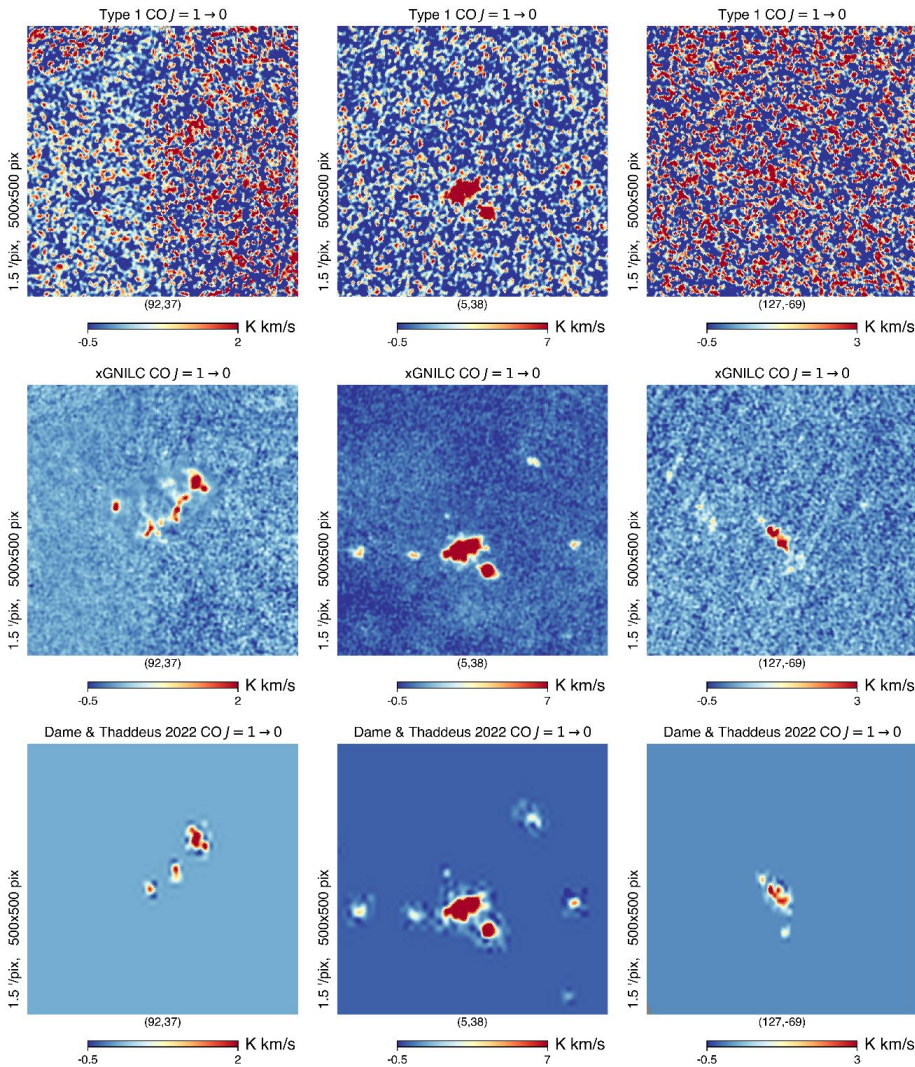
For all pixels  $> 0.1$  K km/s  
the correlation coefficient  
with Dame & Thaddeus  
2022 North Sky Survey is  
0.91

All maps  
smoothed to  
10 arcmin

Dame & Thaddeus 2022  
CO J=1-0

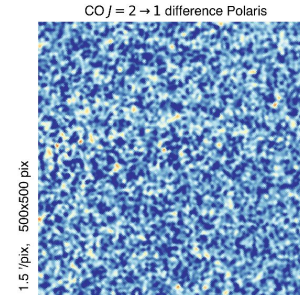
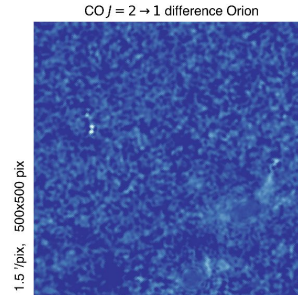
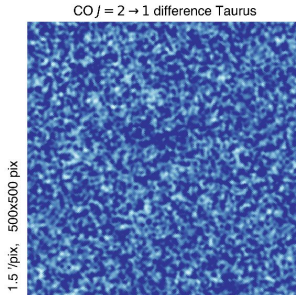
Type-1  
CO J=1-0

xGNILC  
CO J=1-0



# CO 2-1

Type-1 - xGNILC  
CO J=2-1



-1 12 K km/s

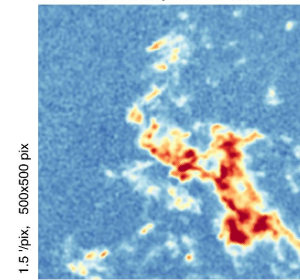
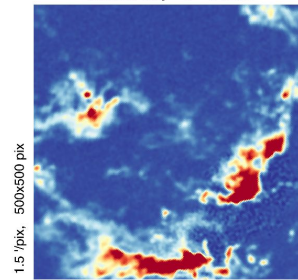
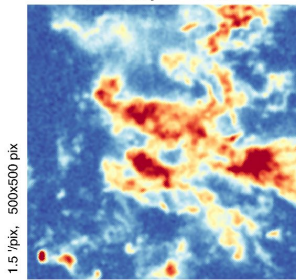
-1 25 K km/s

-1 5 K km/s

xGNILC CO J = 2 → 1 Taurus

xGNILC CO J = 2 → 1 Orion

xGNILC CO J = 2 → 1 Polaris



-1 12 K km/s

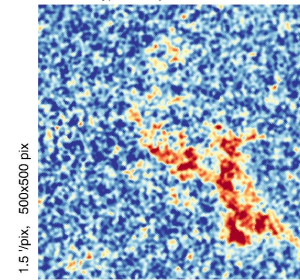
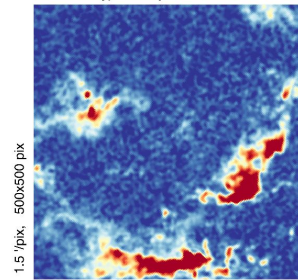
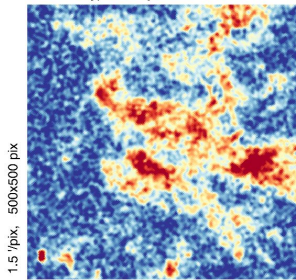
-1 25 K km/s

-1 5 K km/s

Type 1 CO J = 2 → 1 Taurus

Type 1 CO J = 2 → 1 Orion

Type 1 CO J = 2 → 1 Polaris



-1 12 K km/s

-1 25 K km/s

-1 5 K km/s

Type-1  
CO J=2-1

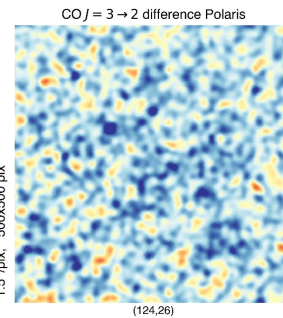
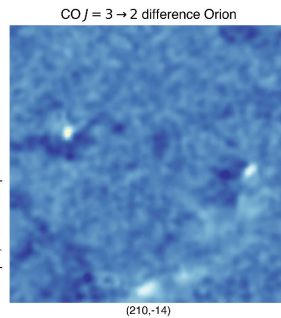
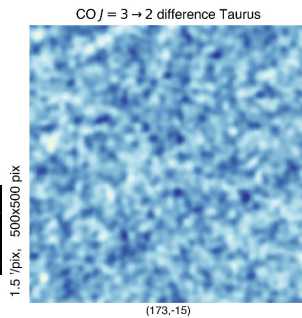
All maps  
smoothed to  
10 arcmin



# CO 3-2

All maps smoothed to 20 arcmin

Type-1 - xGNILC  
CO J=3-2



K km/s

K km/s

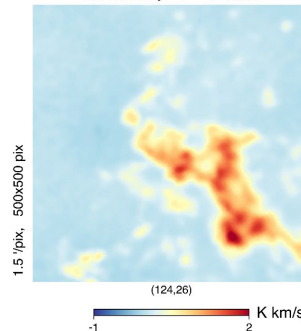
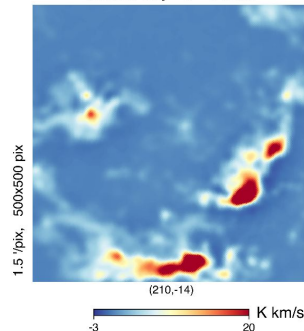
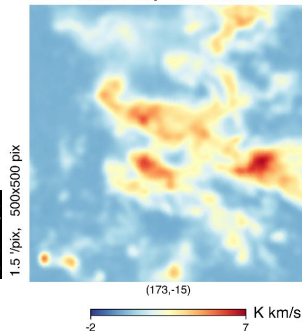
K km/s

xGNILC CO J = 3 → 2 Taurus

xGNILC CO J = 3 → 2 Orion

xGNILC CO J = 3 → 2 Polaris

xGNILC  
CO J=3-2



K km/s

K km/s

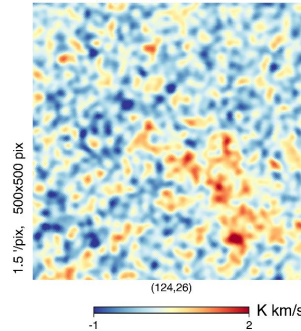
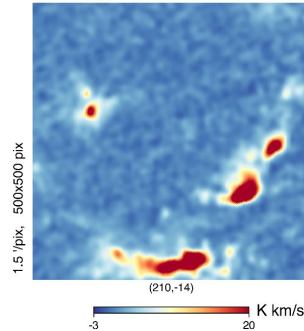
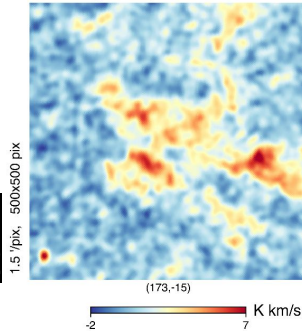
K km/s

Type 1 CO J = 3 → 2 Taurus

Type 1 CO J = 3 → 2 Orion

Type 1 CO J = 3 → 2 Polaris

Type-1  
CO J=3-2



K km/s

K km/s

K km/s

# Summary

- **New low contamination, low noise full sky CO maps from Planck observations.**
- Data products are publicly available from:  
  
[https://portal.nersc.gov/project/cmb/Planck\\_Revisited/co/](https://portal.nersc.gov/project/cmb/Planck_Revisited/co/)
- We plan to update Galactic CO emission models in PySM and PSM using these new maps as templates.



# Appendix

# Type 1 CO map

- Computed from linear combination of individual bolometer maps for a given frequency.
- Exploits the different responses of individual bolometers to the CO line.
- Component separation with a MILCA pipeline which removes certain spectral components while keeping the CO scaling ( $F_{\text{CO}}^{\text{sky}}$ ) for the bolometers intact. Does an ILC.
- Components considered:
  - 100 GHz: CO, CMB(flat scaling)
  - 217 GHz: CO, CMB, dust
  - 353 GHz: CO, dust

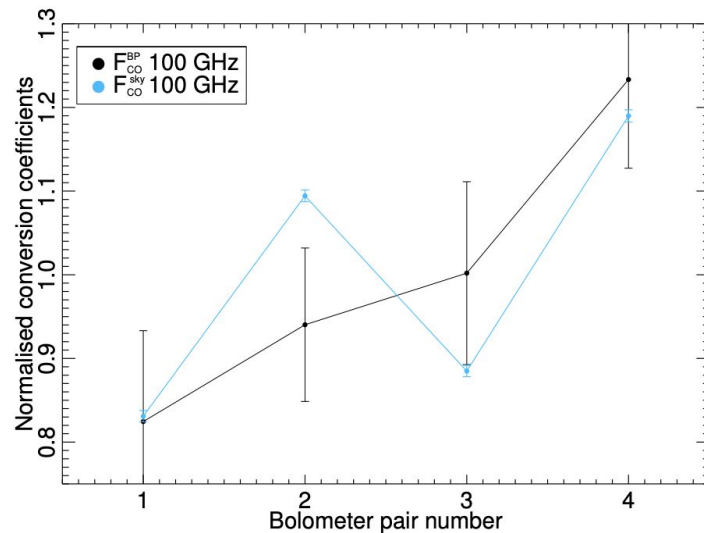
Bolo	ID	$F_{12\text{CO}}^{\text{BP}}$	$F_{13\text{CO}}^{\text{BP}}$	$F_{\text{CO}}^{\text{sky}}$
$J=1 \rightarrow 0$				
100-1	(a+b)/2	$0.82 \pm 0.10$	$1.03 \pm 0.12$	$0.83 \pm 0.01$
100-2	(a+b)/2	$0.94 \pm 0.09$	$0.97 \pm 0.10$	$1.09 \pm 0.01$
100-3	(a+b)/2	$0.99 \pm 0.11$	$0.87 \pm 0.14$	$0.88 \pm 0.01$
100-4	(a+b)/2	$1.24 \pm 0.10$	$1.13 \pm 0.24$	$1.19 \pm 0.01$

individual bolometer map

$$M_b = F_{\text{CO},b}^{\text{fit}} P_{\text{CO}} + F_{\text{dust},b}^{\text{fit}} P_{\text{d}}$$

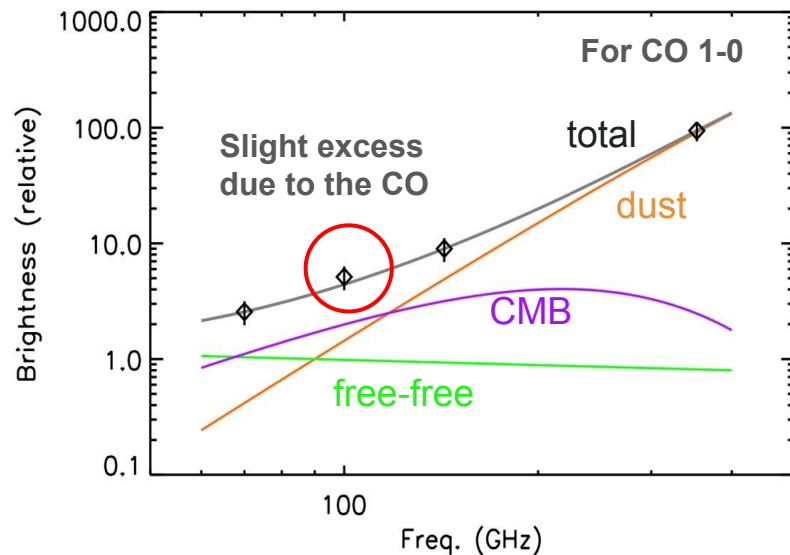
545 GHz as dust template

CO template (Dame)



# Type 2 CO map

- Computed by solving a linear system that assumes 4 emissions components: CO, CMB, free-free and dust
- Employs the Ruler algorithm to obtain a least squares solution.
- Channels used:
  - CO<sub>1-0</sub>: 70 GHz, 100 GHz, 143 GHz and 353 GHz
  - CO<sub>2-1</sub>: 70 GHz, 143 GHz, 217 GHz and 353 GHz
- CMB is modelled as a flat scaling.
- Free-free is modelled as  $\nu^{-2.15}$  power law.
- Dust is modelled as a grey-body with  $T_{\text{dust}}=17$  K and  $\tau_{\text{dust}}=1.6$ .
- All channels reconvolved to common resolution of 15 arcmin.



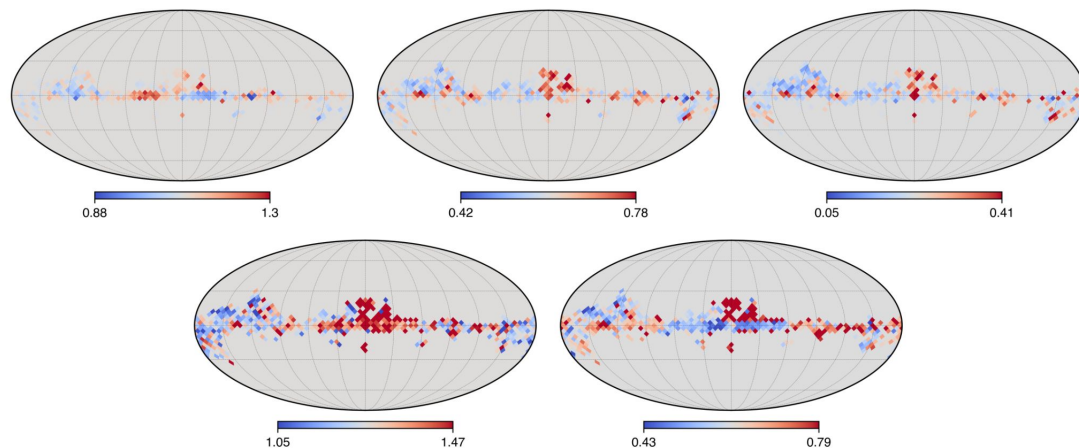
# Calibration

- We fit the CO mixing vector by fitting the following model:

$$\text{CO}_{\text{TypeX}}^J = a_\alpha \text{CO}_{\text{Dame}}^{J=1 \rightarrow 0} + K_{\text{TypeX}}^J$$

- We fit against the Dame et. al. 2001 CO 1-0 map in the Galactic plane.
- The fit is obtained globally or on 30 equal area patches, or on a Healpix NSIDE=16 grid.
- We use the mean of the 30 equal area patches as prior.

Planck map (type and line)	Global fit (with offset)	Mean of 30 (with offset)	Median of 30 (with offset)
TYPE 1 $J = 1 \rightarrow 0$	1.12	$1.09 \pm 0.07$	1.08
TYPE 1 $J = 2 \rightarrow 1$	0.61	$0.60 \pm 0.06$	0.60
TYPE 1 $J = 3 \rightarrow 2$	0.21	$0.23 \pm 0.06$	0.22
TYPE 2 $J = 1 \rightarrow 0$	1.26	$1.26 \pm 0.07$	1.25
TYPE 2 $J = 2 \rightarrow 1$	0.61	$0.61 \pm 0.06$	0.62



# xGNILC pipeline

Assume a data model:

$$\boxed{\text{data}} \quad d = \underbrace{\mathbf{A}t}_{\text{mixing matrix}} + \underbrace{n}_{\text{noise}}$$

signal templates

known covariance  $\mathbf{C}_n$

Noise *whitening* the data:  $d' = \mathbf{C}_n^{-1/2} d$

Covariance of the whitened data :

$$\mathbf{C}_{d'} = [\mathbf{C}_n^{-1/2} \mathbf{A}] \mathbf{C}_t [\mathbf{A}^t \mathbf{C}_n^{-1/2}] + \mathbf{I}$$

Diagonalizing:

$$\mathbf{C}_{d'} = \mathbf{U}[\mathbf{\Lambda} + \mathbf{I}]\mathbf{U}^t$$

We use the Planck CO null maps to estimate the noise covariance.



# xGNILC pipeline

$$\mathbf{C}_{d'} = \mathbf{U} \begin{bmatrix} \lambda_1 + 1 & & & \\ & \ddots & & \\ & & \lambda_n + 1 & \\ & & & \ddots \end{bmatrix} \mathbf{U}^t$$

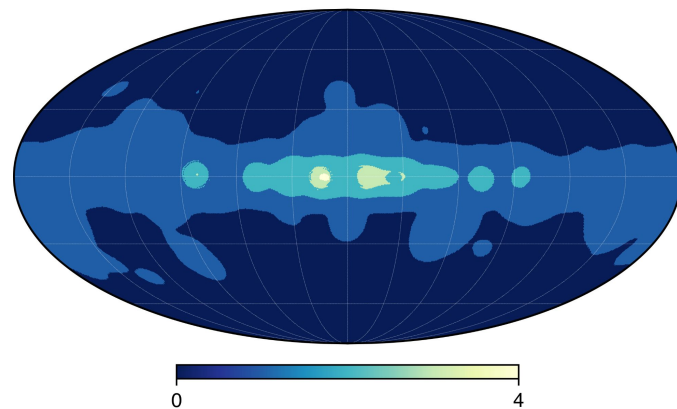
$\lambda_i \gg 1$ :  
significant

$\lambda_i \ll 1$ :  
negligible

Number of significant eigenvalues determine the dimension of the CO signal subspace

Estimate dimensions of the CO signal subspace by minimizing the Akaike Information Criterion:

$$\min_{\alpha \in [1, N_{ch}]} \left[ 2\alpha + \sum_{k=\alpha+1}^{N_{ch}} (\lambda_k - \log \lambda_k - 1) \right]$$



Map of the CO subspace dimension

# xGNILC pipeline

We project the whitened data  $\mathbf{d}'$  on the CO signal subspace spanned the eigenvectors corresponding to the significant eigenvalues. This is an estimate of the whitened CO signal  $\hat{\mathbf{s}}'$ . We undo the noise whitening:  $\hat{\mathbf{s}} = \mathbf{C}_n^{1/2} \hat{\mathbf{s}}'$

Both of these steps are achieved by doing a multidimensional ILC:

$$\hat{\mathbf{s}}_{\text{ILC}} = \hat{\mathbf{A}} [\hat{\mathbf{A}}^t \mathbf{C}^{-1} \hat{\mathbf{A}}]^{-1} \hat{\mathbf{A}}^t \mathbf{C}^{-1} \mathbf{d}$$

Constructed from the significant eigenvectors (and eigenvalues) followed by *de-whitening*

When the signal is below the noise we end up with no significant eigenvalue.

In this case we get a Generalized Least Squares solution using priors on the CO mixing vector.

$$\hat{\mathbf{s}}_{\text{GLS}} = [\mathbf{a}^t \mathbf{C}_n^{-1} \mathbf{a}]^{-1} \mathbf{a}^t \mathbf{C}_n^{-1} \mathbf{d}$$

The priors are computed by fitting Planck CO maps with the Dame et. al. 2001 CO 1-0 map.

# CO 1-0 v dust

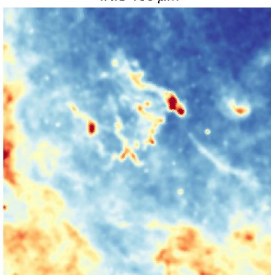
For all pixels  $> 0.1$  K km/s  
the correlation coefficient  
with Dame & Thaddeus  
2022 North Sky Survey is  
0.91

All maps  
smoothed to  
10 arcmin

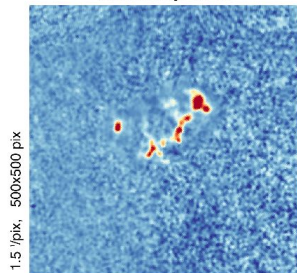
Dame & Thaddeus 2022  
CO J=1-0

IRIS  
100  $\mu\text{m}$

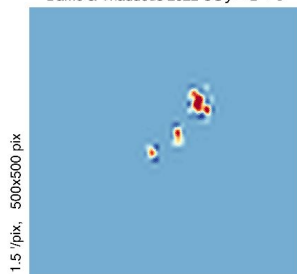
1.5 /pix, 500x500 pix



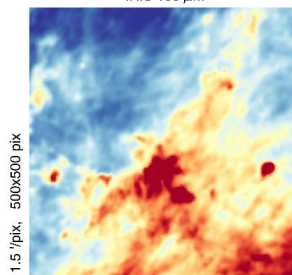
xGNILC CO J = 1  $\rightarrow$  0



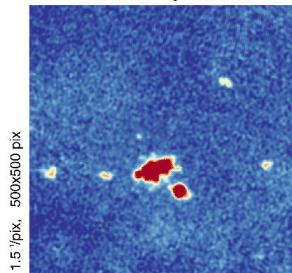
Dame & Thaddeus 2022 CO J = 1  $\rightarrow$  0



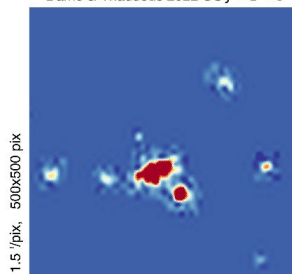
IRIS 100  $\mu\text{m}$



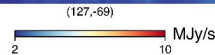
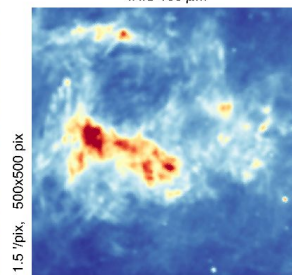
xGNILC CO J = 1  $\rightarrow$  0



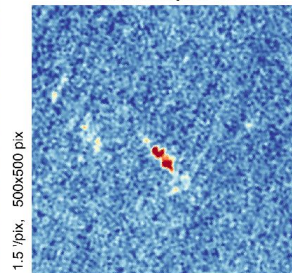
Dame & Thaddeus 2022 CO J = 1  $\rightarrow$  0



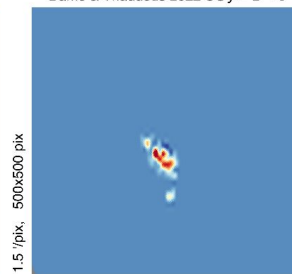
IRIS 100  $\mu\text{m}$



xGNILC CO J = 1  $\rightarrow$  0

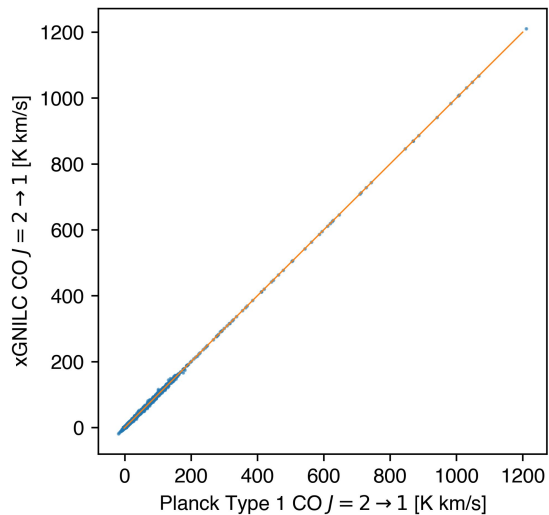


Dame & Thaddeus 2022 CO J = 1  $\rightarrow$  0

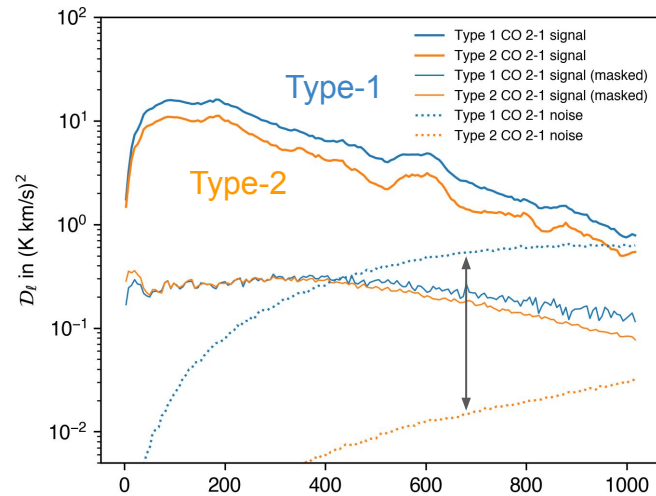
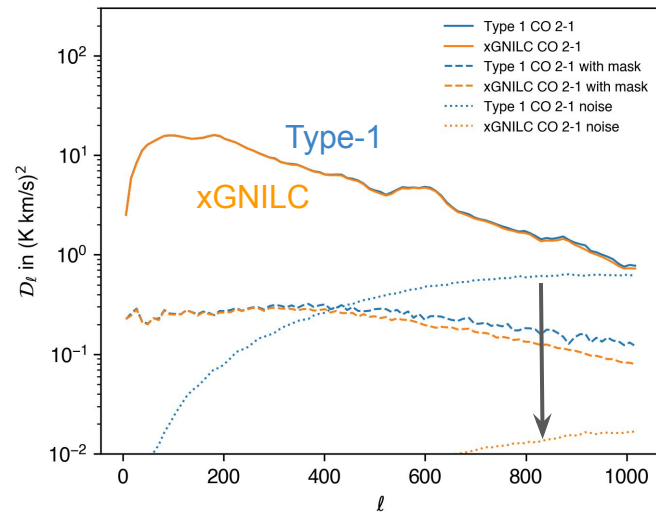
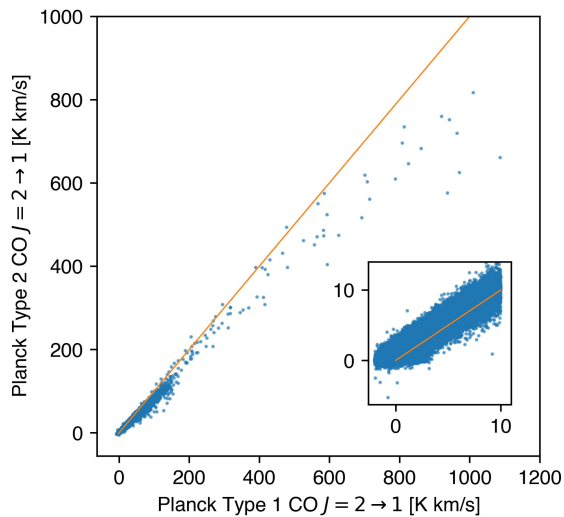


# CO 2-1

CO  $J = 2-1$   
xGNILC vs Type-1

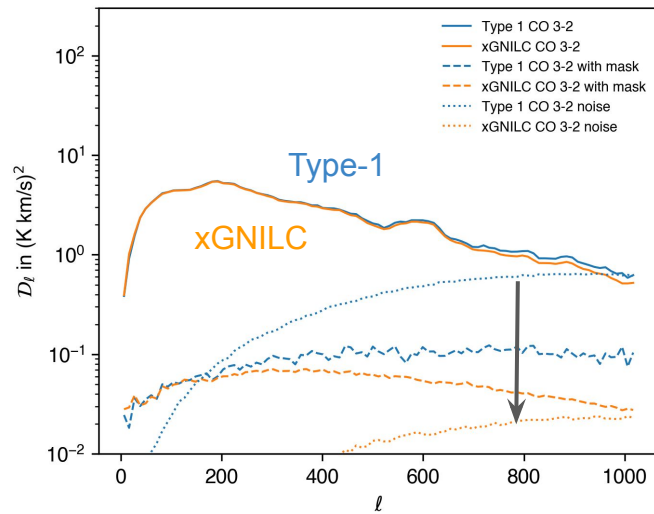
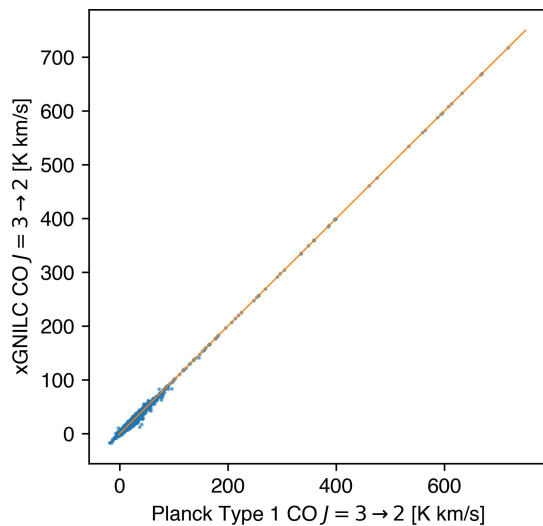


CO  $J = 2-1$   
Type-2 vs Type-1



# CO 3-2

CO  $J = 3-2$   
xGNILC vs Type-1



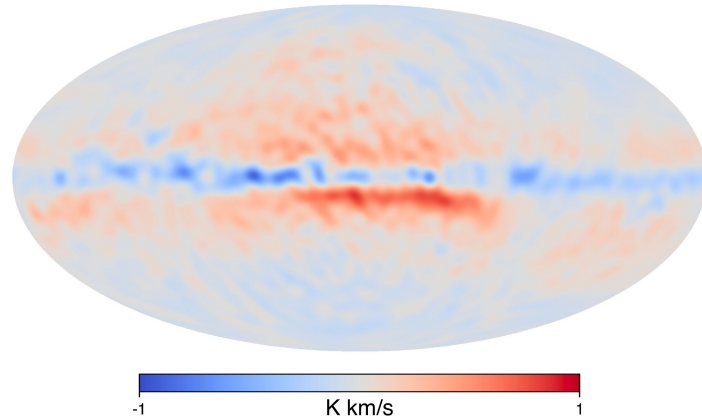
# Post-processing CO 3-2

- Compute residual systematics as:

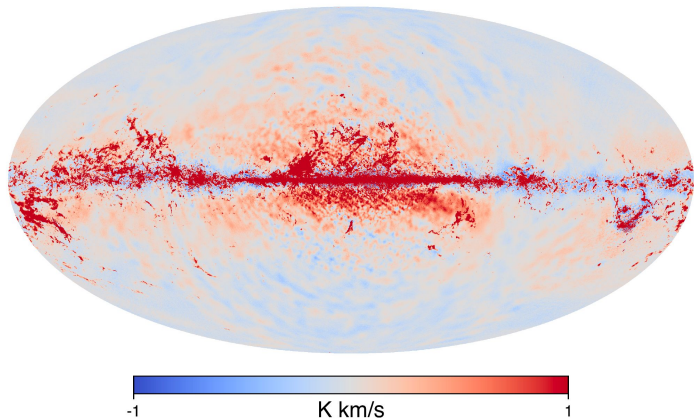
$$\text{CO}_{\text{sys.}}^{3 \rightarrow 2} = \text{CO}_{\text{xGNILC}}^{3 \rightarrow 2} - \frac{a_{3 \rightarrow 2}}{a_{2 \rightarrow 1}} \text{CO}_{\text{xGNILC}}^{2 \rightarrow 1}$$

- Median filter the residual map with galactic plane masking.
- Subtract filtered residual from xGNILC map.

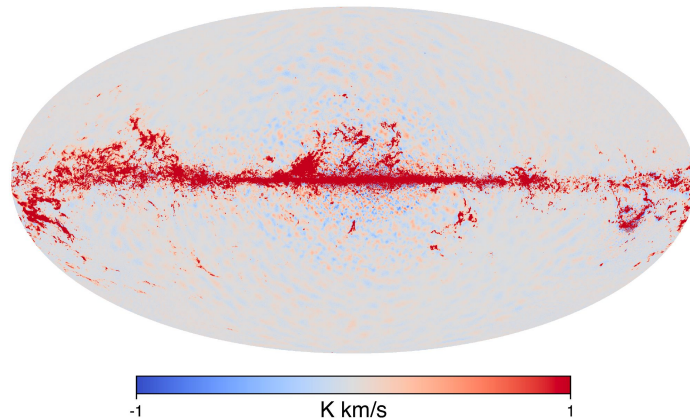
Median of residuals



CO 32



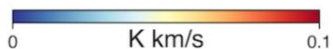
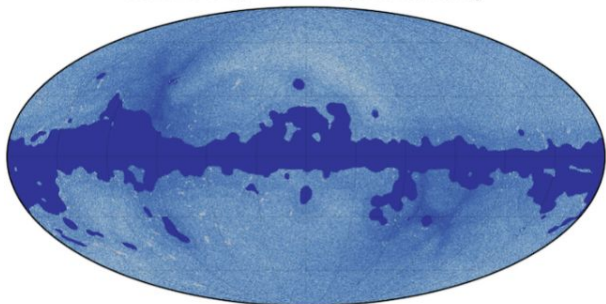
Median filtered CO 32



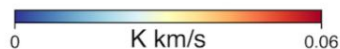
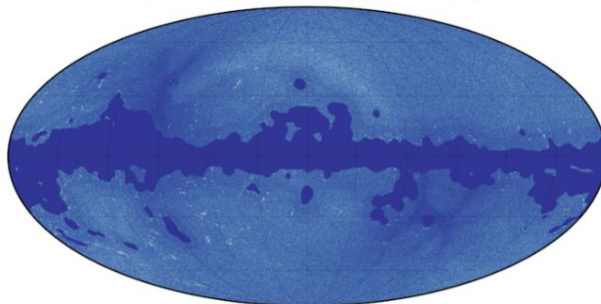
# Systematic Uncertainty

- We construct a multivariate distribution for the input mixing vector prior using the fits to 30 equal area patches.
- Run 200 simulation with input Planck CO maps but replacing the prior used in the GLS step.
- Does not affect the regions where the CO is above the noise (except for CO 3-2).
- Very small systematic uncertainty. CO3-2 uncertainty is higher due to post-processing.

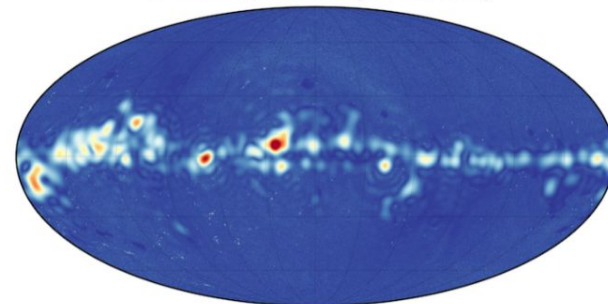
xGNILC CO  $J = 1 \rightarrow 0$  sys. uncertainty



xGNILC CO  $J = 2 \rightarrow 1$  sys. uncertainty



xGNILC CO  $J = 3 \rightarrow 2$  sys. uncertainty

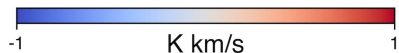
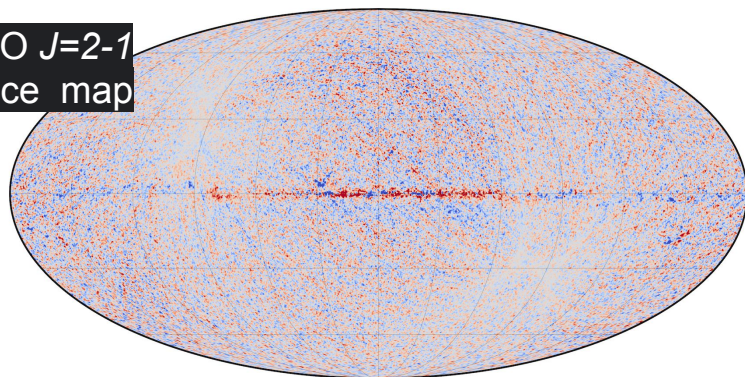


# Difference with input

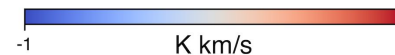
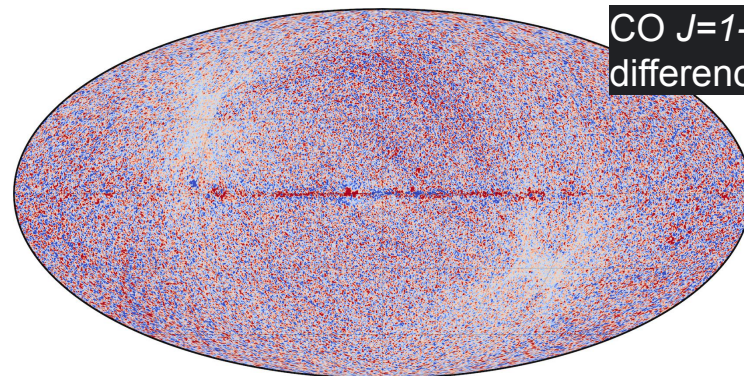
We smooth both xGNILC and Planck Type-I CO maps to 30 arcmin resolution and show the difference as Type-1 - xGNILC.

More difference in the CO 3-2 map due to systematics correction.

CO  $J=2-1$   
difference map



CO  $J=1-0$   
difference map



CO  $J=3-2$   
difference map

